Electric supplementary information (ESI) for:

Unprecedented CO_2 adsorption behaviour by 5A-type zeolite discovered in lower pressure region and at 300 K

Akira Oda,[1] Suguru Hiraki,[1] Eiji Harada,[1] Ikuka Kobayashi,[1] Takahiro Ohkubo,[1] Yuka Ikemoto,[2] Taro Moriwaki[2] and Yasushige Kuroda*[1]

[1]Department of Chemistry, Graduate School of Natural Science and Technology, Okayama University, 3-1-1 Tsushima-naka, Kita-ku, Okayama 700-8530, Japan.

[2]Japan Synchrotron Radiation Research Institute (JASRI), 1-1-1, Kouto, Sayo-cho, Sayo-gun, Hyogo 679-5198, Japan

***Corresponding author e-mail: kuroda@cc.okayama-u.ac.jp**

Experimental

Materials: The 1:1 substitution of Si^{4+} in zeolite by Al^{3+} results in excess negative charges in the lattice, which are balanced by compensating cations that occupy specific sites. In the present case, the Na form of A-type zeolite (NaA; Si/Al =1) purchased from Sigma-Aldrich Co., was used as the starting sample for obtaining the Ca^{2+}-ion-exchanged sample: (NaCaA). The ion-exchanging operation was carried out at 373 K for 4 h in an aqueous solution of $Ca(NO_3)_2$; *ca.* 3 g of zeolite was dispersed into 200 mL of 0. 5 mol/L. This operation was repeated three or five times to obtain the samples with the desired exchanged capacities. The obtained samples were centrifuged and washed thoroughly with distilled water, followed by drying *in vacuo* at RT. The metal contents in the samples were determined by inductively coupled plasma (ICP) analysis (Varian Vista-Pro CCD Simultaneous ICP-ODS: Seiko Instruments & Varian Instruments). The obtained samples were evaluated to have 85% and 65% ion-exchange capacities (called NaCaA-85 and NaCa-65, respectively). Other ion-exchange operations were performed by the same methods by using other $M(NO_3)_2$ samples (M = Mg, Sr, and Ba). Here, the ion-exchange level (%) was estimated by assuming that one divalent cation is exchanged for two monovalent Na ions. We also used the Ca ion-exchanged A-type zeolite sample (Sigma-Aldrich Co.) in this experiment. In this case, the purchased sample was used as is, and its exchange capacity was evaluated to be 78% in our laboratory by applying the ICP method (CaA-78, where the last number indicates the ion-exchange capacity). The following gases used in this work were purchased from GL Sciences Co. (Tokyo, JP): CO_2 (99.9%), CO (99.9%), CH_4 (99.9%), N_2 (99.99%), O_2 (99.9%), and H_2 (99.99%).

Thermogravimetric analysis: Thermogravimetric analysis (TGA) was performed using a ULVAC TGD-9600. The measurements were carried out at a heating rate of 10 K min^{-1} from room temperature to 1273 K under ambient condition. As the typical example, the amount of the NaCaA-85 sample of 10.08 mg was used in the measurement. Judging from this TGA data, all samples used in the present experiment were evacuated at 723 K as the initial treatment. Actually all samples were stable up to *ca.* 1000 K as can be seen from Figure SI-9.

Adsorption measurements: The adsorption isotherms of CO_2 at 298 K were obtained volumetrically using a volumetric adsorption apparatus equipped with an MKS Baratron pressure sensor (type 390). The first adsorption was performed at 298 K on the zeolite treated at 723 K for 4 h under a reduced pressure of 1.3 mPa. After the first run, the zeolites were re-evacuated at 298 K for 4 h, followed by measurement of the second adsorption at 298 K. The first and second heats of adsorption of CO_2 on the NaCaA-85, NaCaA-65, and CaA-78 zeolites were measured at 298 K using a Twin-type Adiabatic Calorimeter, MMC-5111S microcalorimeter (Tokyo-Riko corporation, Tokyo) equipped with a home-made volumetric adsorption apparatus. For examining

the stability of the NaCaA-85 sample, the measurements of adsorption isotherms were also performed several times in the regeneration processes.

Far-IR spectra: In this work, we focused on the exchanged cation-framework vibrational modes being observable in the far-IR region and their shifts upon adsorption. There are some difficulties in obtaining the detailed information from the far-IR region based on the experimental viewpoint. On the experimental basis, we must use polyethylene for the transmittable windows of the light in this region and it is necessary to secure the condition that withstands both lower and higher pressures without leakage. In addition, this material is weak against higher temperatures such as for removing water adsorbed on the zeolite sample. To overcome these difficulties, we designed the *in situ* cell which was available in vacuum and the *in situ* condition after evacuation at higher temperatures. Furthermore, to obtain the information with high sensitivity on the role of exchanged Ca^{2+} ions for the specific CO_2 adsorption observed in the NaCaA-85 zeolite at RT, we measured far-IR spectra in this system by taking advantage of SOR light, which is bright, stable, and reproducible, compared with the conventional IR sources, leading to the precise detection of the definitive change in the cation-vibrational modes of the Ca^{2+}-zeolite vibrations through the adsorption of CO_2 at RT. The measurements in the far-IR region were performed by using the BL43-IR beam line at the SPring-8 facility (Harima, Hyogo Prefecture, Japan) and using the spectrometer Bruker IFS 120 HR (Detector TGS). The Mylar 3.5 μm beam splitter was used in this work, as it was suitable for the spectral regions required here.[1]

Mid-IR spectra: The IR spectra were recorded at RT on a JASCO FT/IR-6600INORG spectrophotometer with a mercury cadmium telluride detector kept at liquid N_2 temperature (accumulation: 256 scans; nominal resolution of 2 cm^{-1}) in the region between 2500–1800 cm^{-1} for the self-supported sample by using an *in situ* cell developed by our group. By contrast, the pelleted sample that is generally used as a self-supporting disk was not suitable for measurement in the low wave-number region because the efficient CO_2 adsorption takes place and gives too strong adsorption to obtain suitable absorption. Therefore, the powdered sample was dispersed in water, and the dispersed solution was added dropwise onto a high-resistivity 10-mm-diameter Si wafer. After drying, the thus-prepared and -supported sample was loaded into an IR cell capable of *in situ* treatments under a reduced pressure of 1 mPa and consecutive *in situ* gas dosage. The IR spectra were recorded between 750–400 cm^{-1} in the transmission mode at RT using a JASCO spectrophotometer equipped with a TGS detector.

TPD: TPD experiments were performed using a TPD-1-AT apparatus (MicrotracBEL Japan, Inc.) with a quadrupole mass analyzer as a detector. First, the NaCaA-85 sample was purged by He (flow rate: 50 mL min^{-1}) at 723 for 4 h, followed by treatment with a gas mixture comprising a 10% CO_2/He mixture at RT for 2h, and subsequently purged at RT with helium gas. To determine the desorption behaviour of adsorbed CO_2 on the NaCaA-85 thus treated, the TPD spectrum was

detected by using a mass spectrometer ($m/z = 44$). The conditions for the TPD measurements were as follows; He was used as the carrier gas at a rate of 30 mL min^{-1}, and the heating rate was 10 K min^{-1} to 973 K.

Breakthrough curve measurements: The CO_2 adsorption and desorption measurements were performed by using two kinds of gas mixtures mimicking atmospheric components made up of CO_2, O_2 and N_2 (0.04%, 20%, and 79.96%, respectively) and also CO_2, CH_4, O_2 and N_2 (0.04%, 0.04%, 20% and 79.92%, respectively). In the respective cases, the NaCaA-85 sample, which had been evacuated at 723 K, was examined in adsorption of the gas mixture at RT, followed by a desorption procedure from RT to 873 K with a heating rate of 10 K min^{-1} on a BELCAT-II (MicrotracBEL Japan, Inc.) with a mass analyzer (BELMass: MicrotracBEL Japan, Inc.) as a detector, at *m/z* values of 44, 32, 28, 16, 15 and 14. To confirm the separation performance of CO_2 in the different conditions as described just above including CH_4 or not, we carried out the different experiments by using N_2 or He as carrier a gas, respectively.

Computational methodology (calculation method)

(1) Calculation conditions. DFT cluster calculations were conducted using the Gaussian 09 program. All calculations were performed at the B3LYP/6-31G(d,p) level with the SCF convergence criterion of 10^{-8} au.

(2) Models.

2-1. Dual Ca^{2+} site: The DFT cluster model of the local environment of a Linde type-A zeolite, i.e., $Al_4Si_{11}O_{16}H_{28}$ geometry that includes the 4-, 6-, and 8-MR sites, was constructed on the basis of the crystallographic data. To meet the charge compensation requirement from the zeolite framework, two Ca ions were placed at the 6-and 8-MR position as counter cations. Geometrical optimization was performed on the coordinates of all atoms except for the framework Si atoms, through which we obtained the cluster model that represents the dual Ca^{2+} sites located at the 6- and 8-MR positions: [^{8MR}Ca, ^{6MR}Ca]-$Al_4Si_{11}O_{16}H_{28}$.

2-2. CO_2 adsorbed on the dual Ca^{2+} site: A CO_2 molecule was placed close to a dual Ca^{2+} site, and the coordinates of all atoms except for the framework Si atoms were optimized. In this optimization process, two local minima were found. One is the CO_2 molecule adsorbed on both two Ca ions in a bridge style: [^{8MR}Ca-(CO_2)-^{6MR}Ca]-$Al_4Si_{11}O_{16}H_{28}$. Other models were the CO_2 molecule adsorbed on only the Ca ion sitting at the 8-MR position and also at the 6-MR position, respectively: [^{8MR}Ca(CO_2), ^{6MR}Ca]-$Al_4Si_{11}O_{16}H_{28}$ and at the 6-MR position[^{8MR}Ca, ^{6MR}Ca(CO_2)]-$Al_4Si_{11}O_{16}H_{28}$ cluster models.

2-3. Vibrational frequency calculations. To reproduce the mid- and far-IR spectra upon the process of CO_2 adsorption on the [^{8MR}Ca, ^{6MR}Ca]-$Al_4Si_{11}O_{16}H_{28}$ cluster model, vibrational frequency calculations were performed on the [^{8MR}Ca, ^{6MR}Ca]-$Al_4Si_{11}O_{16}H_{28}$, [^{8MR}Ca-(CO_2)-^{6MR}Ca]-$Al_4Si_{11}O_{16}H_{28}$, [^{8MR}Ca(CO_2), ^{6MR}Ca]-$Al_4Si_{11}O_{16}H_{28}$, and [^{8MR}Ca, ^{6MR}Ca(CO_2)]-

$Al_4Si_{11}O_{16}H_{28}$ cluster models. In these calculations, terminated H atoms were kept frozen.

Table SI-1a. Physical parameters of some adsorbates.[2]

Molecule	Kinetic diameter / Å	Polarizability / 10^{-25} cm^3	Dipole moment / 10^{-18} esu cm	Quadrupole moment 10^{-26} esu cm^2
CO_2	3.3 —3.9	29.11	0	4.30
CH_4	3.785	25.93	0	0
N_2	3.64—3.80	17.403	0	1.52
O_2	3.467	15.812	0	0.39
H_2	2.827—2.89	8.042	0	0.662
CO	3.690	19.5	0.1098	2.50
NO	3.492	17.0	0.15872	—
N_2O	3.30	30.3	0.16083	—
H_2O	2.641	14.5	1.8546	—

Table SI-1b. Physical parameters of cations.[3]

Molecule	Polarizability / 10^{-25} cm^3	Ionic Radius of Cation / pm	Polarizing Power of Cation (Q/r^2) / 10^{-24} C m^{-2}
Na^+	1.8	102	15.4
Mg^{2+}	0.72	72	61.8
Ca^{2+}	4.71	100	32.0
Sr^{2+}	8.63	118	19.6
Ba^{2+}	15.6	135	17.6

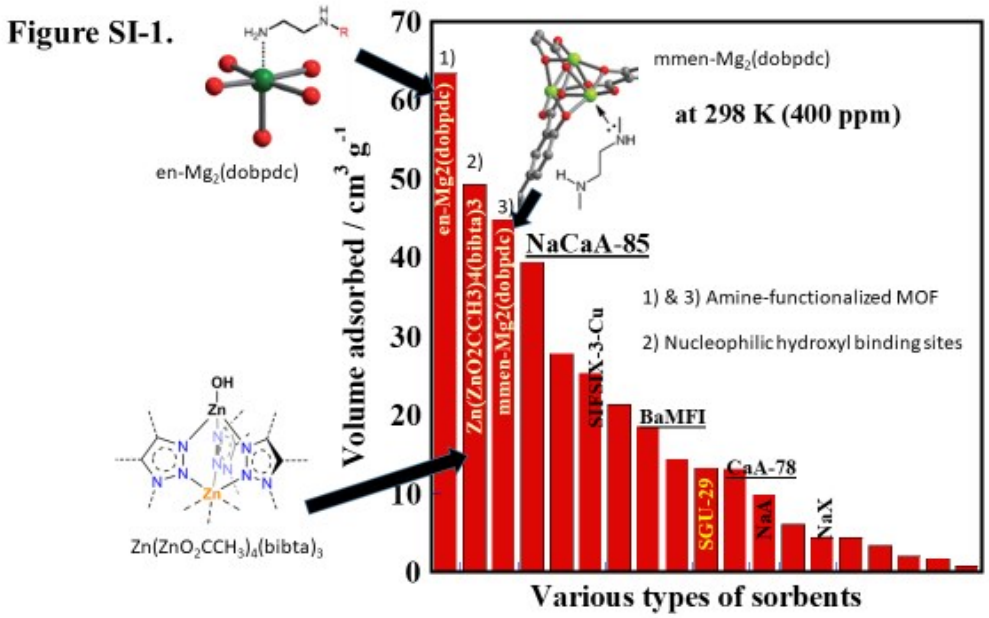

Figure SI-1. Comparison of the adsorbed amounts of CO_2 at 298 K under the pressure of 0. 304 Torr (*ca.* 400 ppm) on various samples.[4–9]

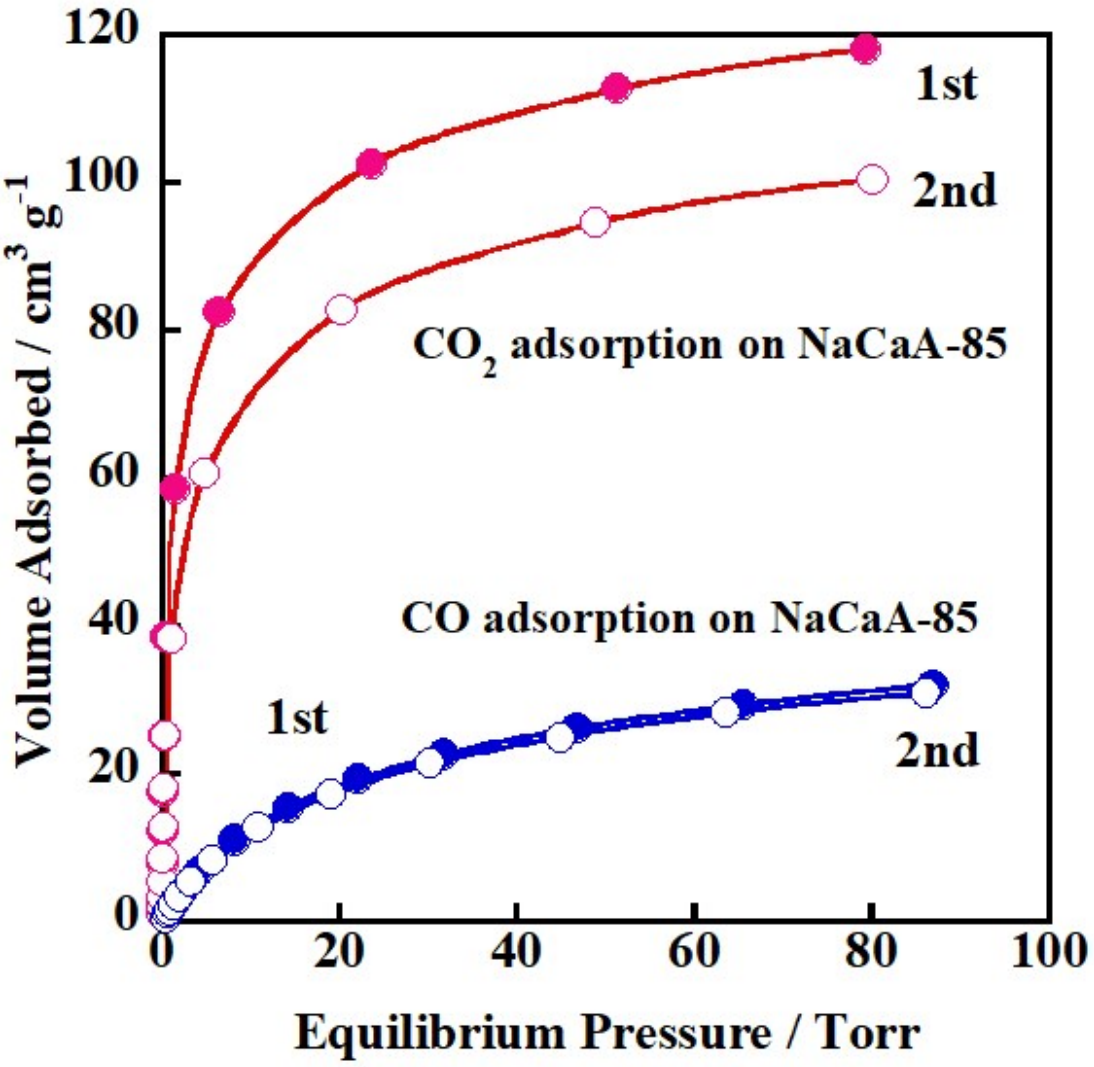

Figure SI-2. Adsorption isotherms of CO_2 and CO at 298 K on the NaCaA-85 sample which was evacuated at 723 K. On these samples the 1st and 2nd isotherms were measured. Solid and open marks correspond to the 1st and 2nd adsorption, respectively; (Red), CO_2 adsorption: (Blue), CO adsorption.

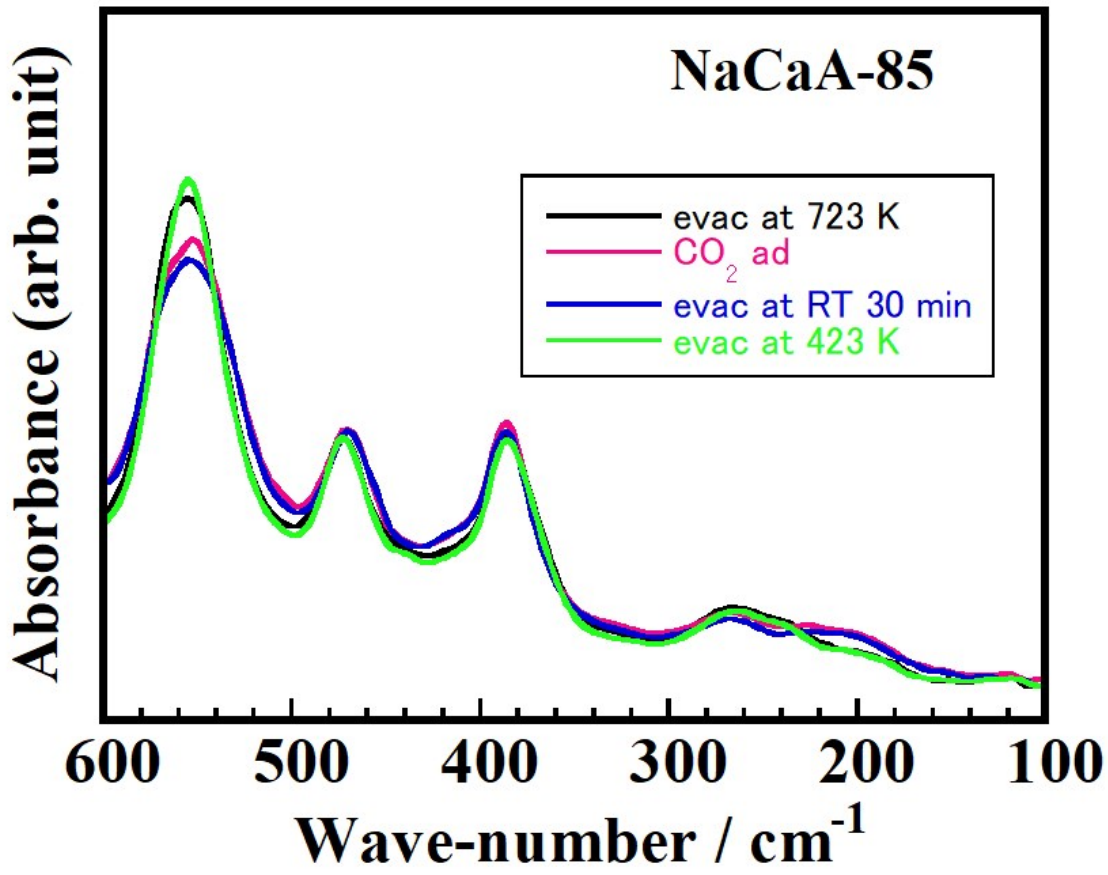

Figure SI-3. Changes in spectra in the far-IR region between 600 and 100 cm^{-1} of the NaCaA-85 sample before and after CO_2 adsorption at RT, and successive evacuation processes at 300 K and 423 K. All measurements were carried out at RT. First all samples were evacuated at 723 K as a standard treatment (black line), followed by equilibrating with CO_2 at RT (Red line), re-evacuation at RT (Blue line), and final re-evacuation at 423 K (Green line), respectively. A series of all treatments were performed under in situ condition.

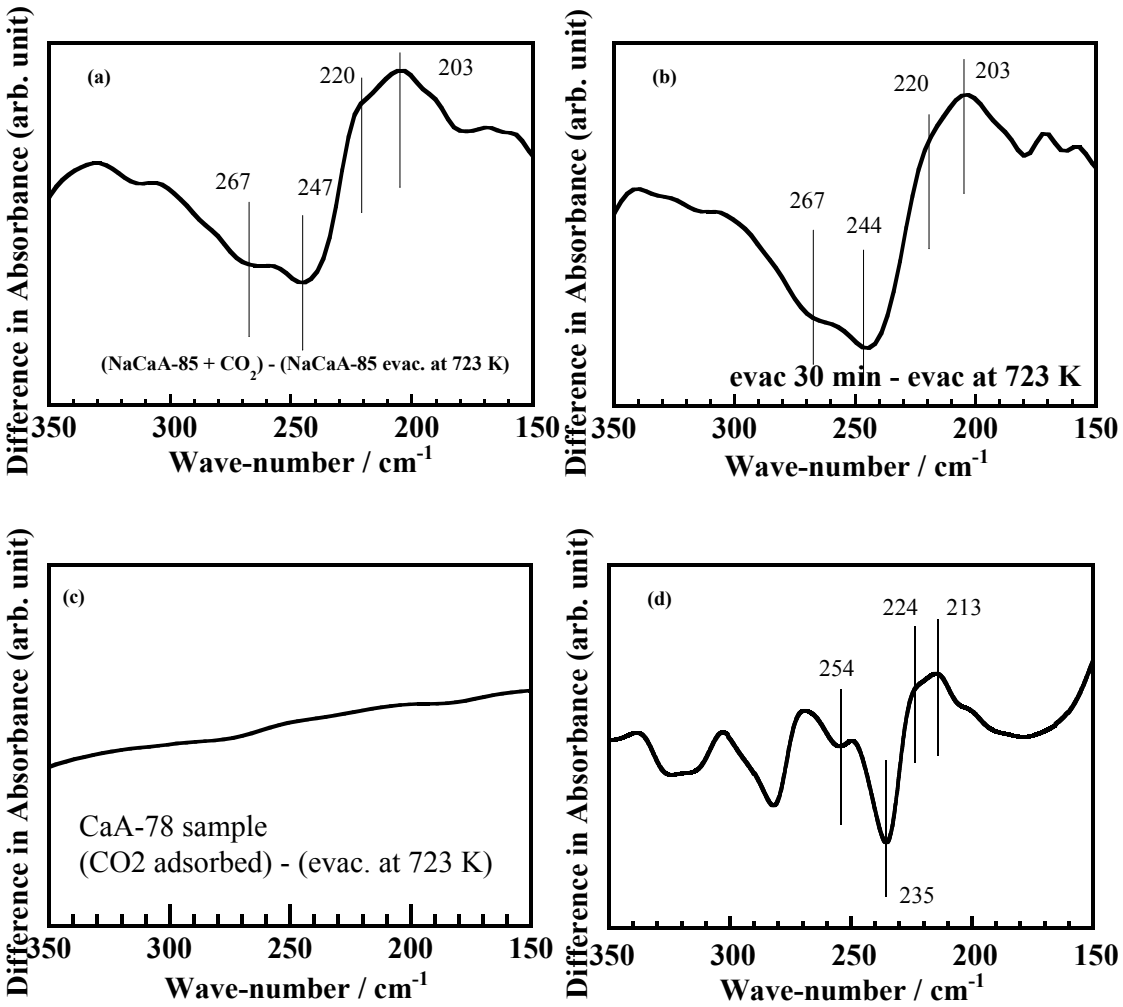

Figure SI-4. The difference spectra in far-IR region before and after CO_2 adsorption on various samples are given in these figures: (a)-(c) are spectra measured experimentally, and (d) is spectrum evaluated with the aid of DFT calculation. (a) The NaCaA-85 sample: difference between the spectrum measured after 723 K and that exposed to CO_2 vapor at RT. (b) The NaCaA-85 sample: difference spectrum between the NaCaA-85 sample measured after evacuating at 723 K and that measured after evacuating at RT of the 723 K-evacuated NaCaA-85 sample followed by exposing to CO_2 vapor at RT of sample. (c) The CaA-78 sample (reference sample): difference spectrum between the CaA-78 sample measured after evacuating at 723 K and that measured after evacuating at RT of the 723 K-evacuated CaA-78 sample followed by exposing to CO_2 vapor at RT of sample.

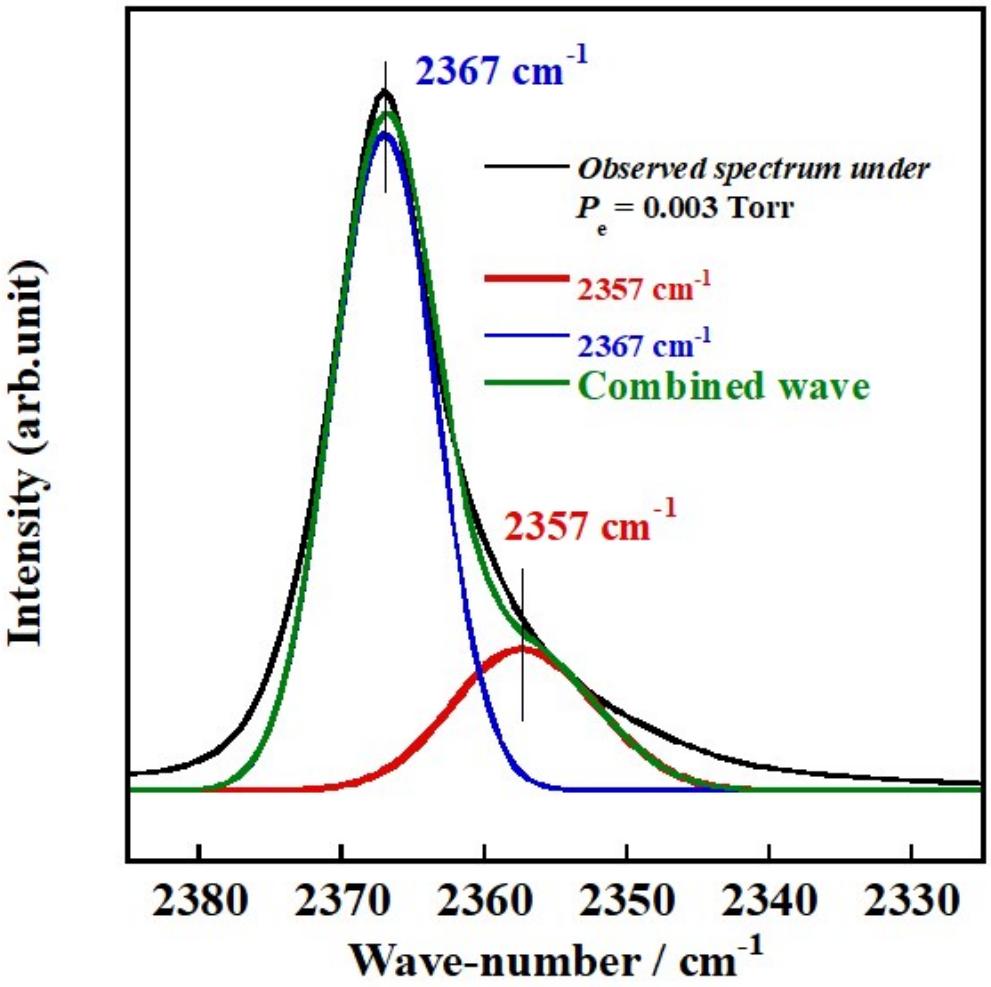

Figure SI-5. The deconvoluted spectrum of the mid-IR spectrum on the CO_2-adsorbed NaCaA-85 sample under extremely low pressure condition. The sample was evacuated at 723 K, followed by CO_2 adsorption at RT.

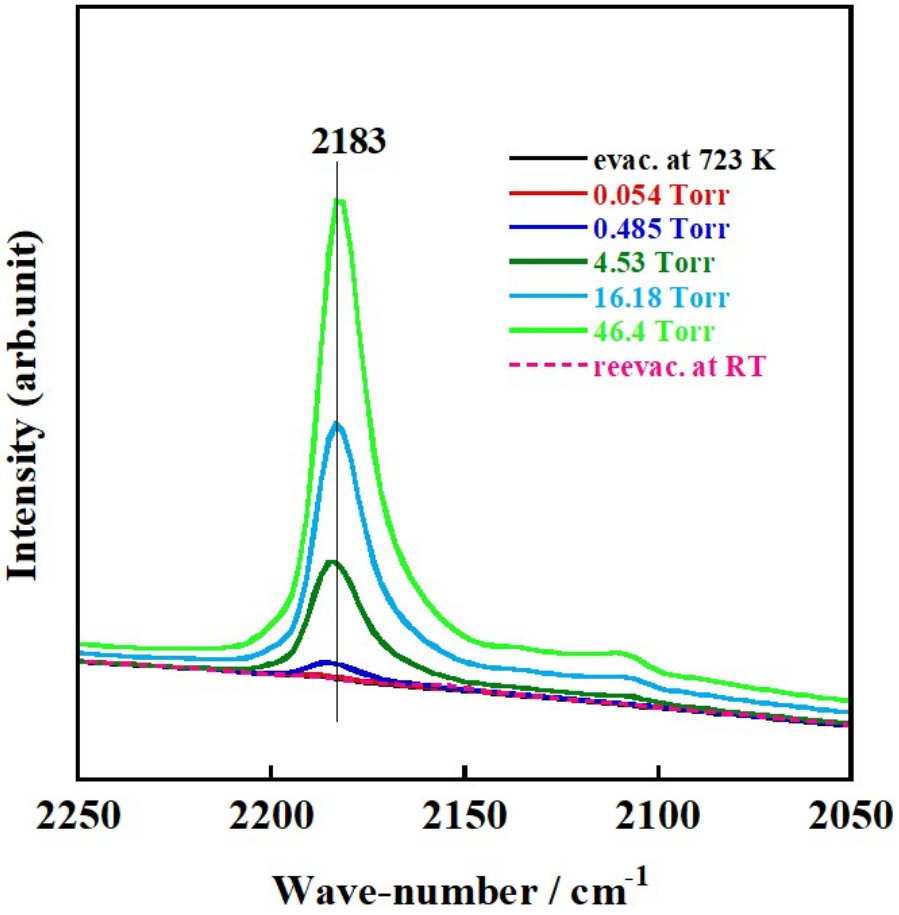

Figure SI-6. IR spectra in the adsorption process of CO at RT under various pressures. This sample was finally evacuated at RT after exposing CO pressure of 46.4 Torr.

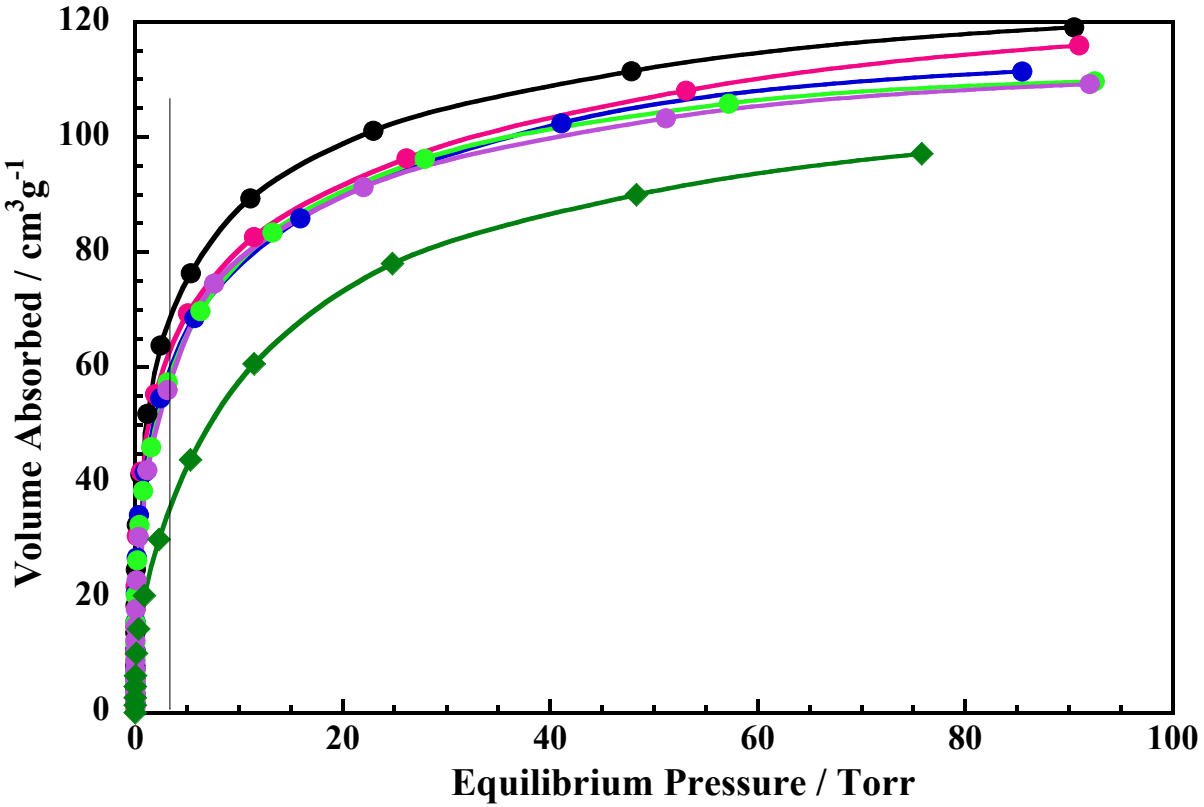

Figure SI-7. Comparison of the 1st isotherms of the original samples with those for the original NaCaA-85 sample (**black circle**) as well as the 1st adsorption on CaA-78 (**dark green diamond**). Regenerated samples through evacuation at 423 K after the CO_2 adsorption: 2nd cycle (**Red** circle), 3rd one (**Blue** circle), 4th one (**Light green** circle), and 5th one (**violet** circle).

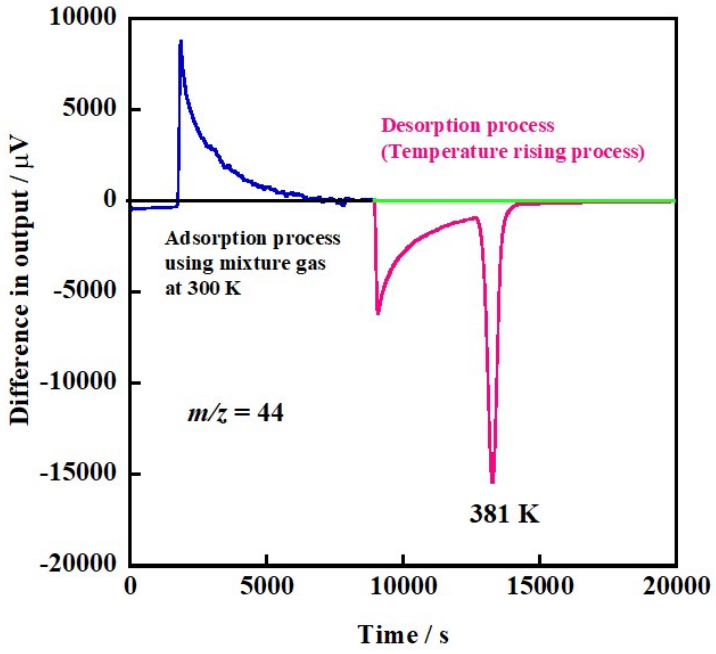

Figure SI-8. Breakthrough curve of CO_2 adsorption and desorption measured by use of a gas mixture mimicking the atmospheric components composed of CO_2, CH_4, O_2, and N_2 (0.04%, 0.04%, 20%, and 79.92%, respectively). The first process corresponds to the change in CO_2 pressure (adsorption) and the second to desorption of adsorbed CO_2. The latter process was composed of two parts; desorption caused by "weakly irreversibly-adsorbed" and "strongly irreversibly-adsorbed" species, respectively.

Figure SI-9 TG data

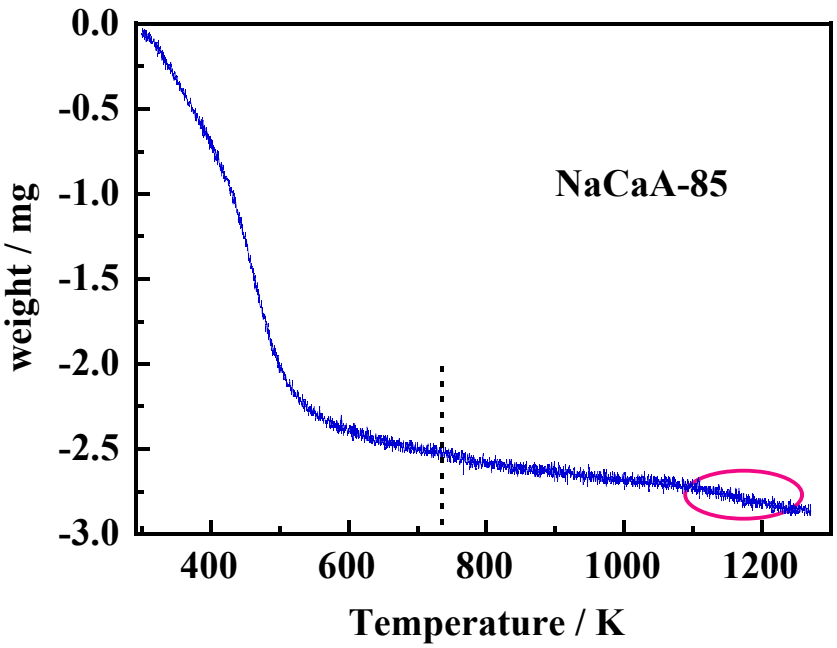

Figure SI-9. DTA data of the NaCaA-85 sample. In this figure, the dashed line indicates the initial evacuation temperature, i.e., 723 K. The decrease in TGA curve was observed in the region surrounded by the red circle which may be ascribed to the starting of the destruction of lattice of 5A-type zeolite.

Reference

1. Y. Ikemoto, T. Moriwaki, T. Nakano and Y. Nozue, Far infrared microspectroscopy of zeolite MOR single crystal. *Infrared Phys. Techn.*, 2006, **49**, 78–81.
2. J.–R. Li, R. J. Kuppler and H.–C. Zhou, Selective gas adsorption and separation in metal–organic frameworks. *Chem. Soc. Rev.,* 2009, **38**, 1477–1504.
3. V. Dimitrov and T. Komatsu, Correlation among electronegativity, cation polarizability, optical basicity and single bond strength of simple oxides. *J. Solid State Chem.,* 2012, **196**, 574-578.
4. en-Mg_2(dobpdc) complex: W. R. Lee, S. Y. Hwang, D. W. Ryu, K. S, Lim, S. S. Han, D. Moon, J. Choi and C. S. Hong, Diamine-functionalized metal-organic framework: exceptionally high CO_2 capacities from ambient air and flue gas, ultrafast CO_2 uptake rate, and adsorption mechanism. *Energy Environ. Sci*., 2014, **7**, 744–751.
5. Biomimetic Zn complex: C. E. Bien, K. K. Chen, S.-C. Chien, B. R. Reiner, L.-C. Lin, C. R. Wade and W. S. Winston Ho, Bioinspired Metal−Organic Framework for Trace CO_2 Capture *J. Am. Chem. Soc.,* 2018, **140**, 12662−12666.
6. mmen-Mg_2(dobpdc) Complex: T. M. McDonald, W. R. Lee, J. A. Mason, B. M. Wiers, C. S. Hong and J. R. Long, Capture of Carbon Dioxide from Air and Flue Gas in the Alkylamine-Appended Metal−Organic Framework mmen-Mg_2(dobpdc). *J. Am. Chem. Soc.,* 2012, **134**, 7056−7065.
7. SIFSIX-3-Cu complex: O. Shekhah, Y. Belmabkhout, Z. Chen, V. Guillerm, A. Cairns, K. Adil and M. Eddaoudi, Made-to-order metal-organic frameworks for trace carbon dioxide removal and air capture. *Nature Commun.,* 2014, **5**, 4228.
8. BaMFI-zeolite: A. Itadani, A. Oda, H. Torigoe, T. Ohkubo, M. Sato, H. Kobayashi and Y. Kuroda, Material Exhibiting Efficient CO_2 Adsorption at Room Temperature for Concentrations Lower Than 1000 ppm: Elucidation of the State of Barium-Ion Exchanged in an MFI-Type Zeolite. *ACS Appl. Mater. Interfaces*, 2016, **8**, 8821–8833.
9. SGU-29: S. J. Datta, C. Khumnoon, Z. H. Lee, W. K. Moon, S. Docao, T. H. Nguyen, I. C. Hwang, D. Moon, P. Oleybujiv, O. Terasaki and K. B. Yoon, CO_2 capture form humid atmosphere using a microporous coppersilicate. *Science*, 2015, **350(6258)**, 302–306.